

Quantum Gates Between Distant Qubits via Spin-Independent Scattering

Leonardo Banchi^{1,2}, Enrico Compagno¹, Vladimir Korepin³, and Sougato Bose¹

¹ Department of Physics and Astronomy, University College London, Gower St., London WC1E 6BT, UK

² QOLS, Blackett Laboratory, Imperial College London, SW7 2AZ, UK

³C. N. Yang Institute for Theoretical Physics, State University of New York at Stony Brook, NY 11794-3840, USA

November 30, 2017

We show how the spin independent scattering of two initially distant qubits, say, in distinct traps or in remote sites of a lattice, can be used to implement an entangling quantum gate between them. The scattering takes place under 1D confinement for which we consider two different scenarios: a 1D wave-guide and a tight-binding lattice. We consider models with contact-like interaction between two fermionic or two bosonic particles. A qubit is encoded in two distinct spins (or other internal) states of each particle. Our scheme enables the implementation of a gate between two qubits which are initially too far to interact directly, and provides an alternative to photonic mediators for the scaling of quantum computers. Fundamentally, an interesting feature is that “identical particles” (e.g., two atoms of the same species) and the 1D confinement, are both necessary for the action of the gate. Finally, we discuss the feasibility of our scheme, the degree of control required to initialize the wave-packets momenta, and show how the quality of the gate is affected by momentum distributions and initial distance. In a lattice, the control of quasi-momenta is naturally provided by few local edge impurities in the lattice potential.

1 Introduction

Recent progress in the control of the motion of neutral atoms in restricted geometries such as traps [1, 2, 3, 4], 1D optical lattices [5, 6, 7] and wave-guides [8] has been astounding. Naturally, the question arises as to whether they

can be used in a similar manner as photons are used, i.e., as “flying qubits” for logic as well as for connecting well separated registers in quantum information processing. Quantum logic between flying qubits exploits their indistinguishability and assume them to be *mutually non-interacting* – hence the names “linear optics” [9] and “free electron” [10] quantum computation. In fact, for such an approach to be viable one has to engineer circumstances so that the effect of the inter-qubit interactions can be ignored [11]. On the other hand, in the context of photonic qubits, it is known that effective interactions, engineered using atomic or other media, may enhance the efficacy of processing information [12, 13, 14, 15, 16]. One is thereby motivated to seek similarly efficient quantum information processing (QIP) with material flying qubits which have the advantage of *naturally interacting* with each other. Further motivation stems from the fact that for non-interacting mobile fermions, additional “which-way” detection is necessary for quantum computation [10] and even for generating entanglement [17], which are not necessarily easy. Thus, if interactions do exist between flying qubits of a given species, one should aim to exploit these for QIP.

While it is known that both spin-dependent [18] and spin-independent [19, 20, 21, 22] scattering can entangle, it is highly non-trivial to obtain a useful quantum gate. The amplitudes of reflection and transmission in scattering generally depend on the internal states of the particles involved which makes it difficult to ensure that a unitary operation i.e., a quantum gate acts exclusively on the limited logical (e.g. internal/spin) space that encodes the qubits. For non-identical (one static and one mobile) particles, it has been

arXiv:1412.3582v4 [quant-ph] 29 Nov 2017

shown that a quantum gate can be engineered from a spin dependent scattering combined with an extra potential [23]. An alternative approach is based on collision between matter-wave solitons that can be used to generate entanglement between them [24]. We will show here that one can accomplish a quantum gate merely from the spin independent elastic scattering of two identical particles. This crucially exploits quantum indistinguishability, as well as the equality of the incoming pair and outgoing pair of momenta in one dimension (1D). In our scheme the quantum gate is only dictated by the Scattering matrix or *S-matrix* acting on the initial state of the two free moving qubits. This is thus an example of *minimal control* QIP where nothing other than the initial momenta of the qubits is controlled. Not only will it enable QIP beyond the paradigm of linear optics with material flying qubits, but also potentially connect well separated registers of static qubits. One static qubit from each register should be out-coupled to momenta states in matter wave-guides and made to scatter from each other. The resulting quantum gate will connect separated quantum registers. This may be simpler than interfacing static qubits with photons.

While quantum gates exploiting the mutual interactions of two material flying qubits have not been considered yet in full detail, the corresponding situation for *static* qubits has been widely studied (e.g., Refs.[25, 26, 27, 28, 29, 30, 31, 32]). However, these methods typically require a precise control of the interaction time of the qubits or between them and a mediating bus (e.g., Refs.[33, 34, 35]). Still static qubits offer the natural candidate for information storage. Motivated by this, and also by the high degree of control reached in current optical lattice experiments [5, 6], as a second result of this paper we consider a lattice implementation of our gate. A scattering based approach for creating entanglement in lattice setups was considered in [36], though they assume periodic boundaries, which are difficult to achieve, and a careful initialization and control of the particles' momenta. On the other hand, our method exploits a much lower control process, as the control of quasi-momenta is naturally provided by few local edge impurities in the lattice potential. This experimental proposal is particularly compelling also because the qubit can be

made either static or mobile depending on the tunable potential barrier on different lattice sites, thus avoiding to seek some mechanism to couple static and mobile particles and allowing for both storage and computation with the same physical setup.

Our study interfaces QIP and quantum indistinguishability with two other areas, namely the Bethe-Ansatz exact solution of many-body models [37] and the 1D confinement of atoms already achieved in experiments [38, 39, 40, 44, 45, 46, 47, 48, 49, 50, 51, 6].

2 Quantum gate between flying qubits

A two qubit entangling gate is important as it enables universal quantum computation when combined with arbitrary one qubit rotations [52]. We consider the spin independent interaction to be a contact interaction between point-like non-relativistic particles. For two *spinless* bosons on a line (1D) the Hamiltonian with a delta-function interaction is [37]

$$H = -\frac{\partial^2}{\partial x_1^2} - \frac{\partial^2}{\partial x_2^2} + 2c\delta(x_1 - x_2), \quad (1)$$

where x_1 and x_2 are the coordinates of the two particles. The above model is called the Lieb-Liniger model and has an interesting feature which we will actively exploit. This is the fact that the momenta are individually conserved during scattering. If the incoming particles have momenta p_1 and p_2 , then the outgoing particles *also* have momenta p_1 and p_2 [53], as shown in Fig.1(a). Thus the scattering matrix is diagonal in the basis of momenta pairs and is, in fact, only a phase which accumulates on scattering. The scattering matrix extracted from these wavefunctions is given, for incident particles with momenta $p_2 > p_1$, by [37]

$$S(p_2, p_1) = \frac{p_2 - p_1 - ic}{p_2 - p_1 + ic}. \quad (2)$$

The phase accumulated on scattering is $-i \ln S(p_2, p_1)$. Note that, as expected, for non-interacting bosons ($c \rightarrow 0$), their exchange causes no phase change, while when $c \rightarrow \infty$ (impenetrable bosons equivalent to free fermions) have a -1 factor multiplying on exchange.

We consider the case of colliding particles having some internal degrees of freedom in which a

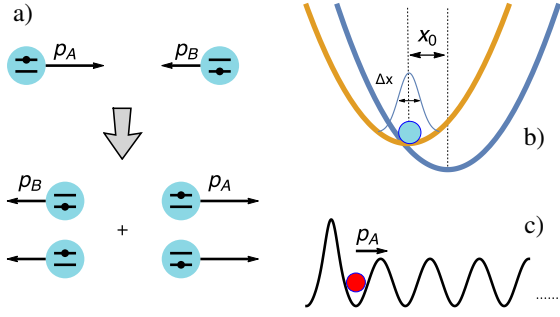


Figure 1: (color online) Part (a) shows the nature of 1D scattering of two identical particles, labeled as A and B according to their momenta directions, where some internal states encode the logical states of the qubit. Incoming particles of momenta p_A and p_B imply outgoing particles of exactly the same momenta. Their internal degrees of freedom on the other hand get entangled after the collision. Part (b) and (c) shows two different physical implementations of the scheme depicted in part (a). Part (b) deals with flying qubits, where a momentum p is obtained via suitably controlled local traps. Part (c) considers an optical lattice implementation, where a higher barrier on the left forces the qubit to travel to the right.

qubit can be encoded (Fig.1(a)). The collision is assumed to have the form of a *spin independent* contact (delta) interaction of point-like particles as in Eq.(1). We first consider bosons with two relevant states $|\uparrow\rangle$ and $|\downarrow\rangle$ of some internal degree of freedom (could be any two spin states of a spin-1 boson, for example), and define the swap (permutation) operator Π_{12} on the internal (spin) degrees of freedom as $\Pi_{12}(|u\rangle_1|v\rangle_2)=|v\rangle_1|u\rangle_2$, where $|u\rangle_1$ and $|v\rangle_2$ are arbitrary spin states of the particles – so Π_{12} is a 4×4 matrix. From the swap operation we can construct the projectors on the symmetric (+) and antisymmetric (-) subspaces as $\Pi_{\pm} = (1 \pm \Pi_{12})/2$. For symmetric states of the internal degrees of freedom, namely eigenvectors of Π_{12} with eigenvalue 1, the external degrees of freedom also have to be symmetric and have the *same* scattering matrix as spinless bosons (2). On the other hand, for antisymmetric spin states, the spatial wave function of the two particles is fermionic so that the amplitude for $x_1=x_2$ (the chance of a contact delta interaction) is zero implying that they do not scatter from each other. The above observations lead to the S-matrix $S^B(p_2, p_1) = S(p_2, p_1)\Pi_+ + \Pi_-$, namely (for $p_2 > p_1$)

$$S^B(p_2, p_1) = \frac{(p_2 - p_1) - ic\Pi_{12}}{p_2 - p_1 + ic}. \quad (3)$$

We also consider the case where qubit states are spin states of a spin-1/2 particle (say, electrons or fermionic atoms). This is the conventional encoding in many quantum computation schemes. In this case the S -matrix was computed by C. N. Yang [54] to be (for $p_2 > p_1$)

$$S^F(p_2, p_1) = \frac{p_2 - p_1 + ic\Pi_{12}}{p_2 - p_1 + ic}. \quad (4)$$

We consider a frame in which two qubits are moving towards each other, so that after some time they interact with the spin-independent interaction (1). Let us call the qubit with momentum towards the *right* as qubit A , while the qubit with momentum towards the *left* is called qubit B . Each qubit is in a definite momenta state, whose magnitudes are p_A and p_B respectively [55]. Thus $p_2 = p_A$ and $p_1 = -p_B$. The evolution of the 4 possible qubit states due to the scattering is thereby given by

$$\begin{aligned} S^{B/F}|\uparrow\rangle_A|\uparrow\rangle_B &= e^{i\phi_{B/F}}|\uparrow\rangle_A|\uparrow\rangle_B \\ S^{B/F}|\downarrow\rangle_A|\downarrow\rangle_B &= e^{i\phi_{B/F}}|\downarrow\rangle_A|\downarrow\rangle_B \\ S^{B/F}|\uparrow\rangle_A|\downarrow\rangle_B &= \frac{p_{AB}|\uparrow\rangle_A|\downarrow\rangle_B \mp ic|\downarrow\rangle_A|\uparrow\rangle_B}{p_{AB} + ic} \\ S^{B/F}|\downarrow\rangle_A|\uparrow\rangle_B &= \frac{p_{AB}|\downarrow\rangle_A|\uparrow\rangle_B \mp ic|\uparrow\rangle_A|\downarrow\rangle_B}{p_{AB} + ic} \end{aligned} \quad (5)$$

where $p_{AB} = p_A + p_B$, $e^{i\phi_B} = \frac{p_{AB} - ic}{p_{AB} + ic}$ and $e^{i\phi_F} = 1$. Unless either p_{AB} or c vanishes, the above is manifestly an entangling gate, as is evident from the fact that the right hand sides of the last two lines of Eq. (5) is an entangled state. This gate is the most entangling (i.e., the most useful in context of quantum computation, equivalent in usefulness to the well known Controlled NOT or CNOT gate) when $p_{AB} \approx c$, as then the right hand sides of the last two lines of Eq. (5) correspond to maximally entangled states $\frac{e^{-i\frac{\pi}{4}}}{\sqrt{2}}(|\uparrow\rangle_A|\downarrow\rangle_B \mp i|\downarrow\rangle_A|\uparrow\rangle_B)$ and $\frac{e^{-i\frac{\pi}{4}}}{\sqrt{2}}(|\downarrow\rangle_A|\uparrow\rangle_B \mp i|\uparrow\rangle_A|\downarrow\rangle_B)$ respectively. The above gates would aid universal quantum computation by means of scattering with both bosonic and fermionic qubits. The gates of Eqs.(5) are easiest to exploit as the only other requirement, namely local rotations of the qubit states are accomplishable by means of laser induced transitions between different atomic internal levels or electronic spin rotations by magnetic fields.

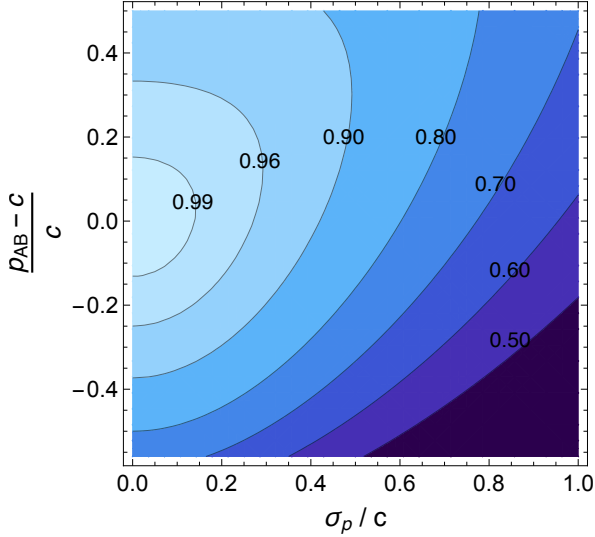


Figure 2: Concurrence between internal (spin) degrees of freedom for two Gaussian wave-packets, when the relative momentum $p_2 - p_1$ is peaked around p_{AB} with width σ_p , and $c > 0$. Numbers indicate the value of the concurrence for those contours.

2.1 Error estimates for extended packets

The amplitudes in Eqs.(5) depend only on the ratio of p_{AB}/c and thereby any spread δp_{AB} of the relative momenta of the incoming particles only affects the amplitudes as $\delta p_{AB}/c$. As a relevant example we consider two Gaussian wavepackets in the internal state $|\uparrow\rangle_A |\downarrow\rangle_B$. Since the center of mass and relative coordinates are decoupled in Eq. (1) we assume that the Gaussian packet can be factorized as $\tilde{\psi}(p_{c.m.})\psi(p)$ where $p = p_2 - p_1$ and $p_{c.m.} = (p_2 + p_1)/2$. The wave-function $\tilde{\psi}(p_{c.m.})$ can be ignored, as it provides only a global phase, while $\psi(p)$ is a Gaussian wave packet centered around p_{AB} with variance σ_p . After the scattering, the state is

$$|\psi\rangle = \int dp \psi(p) \frac{p |\uparrow_A \downarrow_B; p\rangle \mp ic |\downarrow_A \uparrow_B; p\rangle}{p + ic}. \quad (6)$$

The entanglement between the internal degrees of freedom in the scattered state can be measured by the concurrence [56, 57] C . After a partial trace over the momentum, one finds that $C = |\int |\psi(p)|^2 \frac{2cp}{p^2 + c^2} dp|$, namely $C = |2\Re[z]\Im[f(z)]|$, where $z = \frac{c - ip_{AB}}{\sqrt{2}\sigma_p}$ and $f(z) = \sqrt{\pi} e^{z^2} \operatorname{erfc}(z)$. From the asymptotic expansion [58] $zf(z) \approx 1 - z^{-2}/2$ one obtains that C slowly decays as a function of $\delta = (p_{AB} - c)/c$ and σ_p/c , and that the case $\delta \gtrsim 0$ is less prone to errors when σ_p increases – see also Fig. 2. Er-

rors can thereby be *arbitrarily reduced* in principle by choosing particles with higher c . This is opposite to the usual paradigm of gates based on “timed” interactions, where for a given timing error δt , stronger interactions enhance the error (while weaker interactions make gates both slower and susceptible to decoherence).

2.2 Explicit time dependence

In the previous section we used the scattering matrix formalism, which works in the asymptotic regime. Here we work out the time and space dependence more explicitly, focusing on the bosonic case, though a similar analysis can be performed also for fermionic particles. By introducing the relative $x_r = x_1 - x_2$ and central $x_m = x_1 + x_2$ coordinates we see that the Hamiltonian (1) can be written as $H = -2\frac{\partial^2}{\partial x_m^2} - 2\frac{\partial^2}{\partial x_r^2} + 2c\delta(x_r)$, where x_m and x_r are decoupled. As noted in the previous section, the evolution in the symmetric and anti-symmetric subspaces differ only by the interaction term – for exclusion principle the δ interaction is effectively zero in the anti-symmetric space. Therefore, in these two subspaces the central coordinates have the same evolution and can therefore be ignored. In the anti-symmetric subspace the relative coordinates evolve without δ interaction and therefore their dynamics is described [59] by the propagator $G_t(x, y) = \frac{1}{\sqrt{8\pi it}} \exp\left(\frac{i(x-y)^2}{8t}\right)$. Calling $\psi_0(y_r)$ is the initial wavefunction at $t = 0$, then the evolved wave-packet in the anti-symmetric space is $\psi_t^-(x_r) = \int G_t(x_r, y_r) \psi_0(y_r) dy_r$. On the other hand, in the symmetric subspace the particles feel the interaction and the evolved wavefunction [59] is $\psi_t^+(x_r) = \psi_t^-(x_r) + \hat{\psi}_t(x_r)$ where $\hat{\psi}_t(x_r) = \int \hat{G}_t(x_r, y_r) \psi_0(y_r) dy_r$, and

$$\hat{G}_t(x, y) = -\frac{c}{2} \int_0^\infty e^{-cu/2} G_t(|x| + |y| + u, 0) du. \quad (7)$$

If the two particles are initially in the product state $|\uparrow_A \downarrow_B\rangle$, then at time t they are in the state

$$|\psi_t\rangle = \int dy \left[\psi_t^-(y) + \frac{\hat{\psi}_t(y)}{2} |\uparrow_A \downarrow_B; y\rangle + \frac{\hat{\psi}_t(y)}{2} |\downarrow_A \uparrow_B; y\rangle \right]. \quad (8)$$

After a partial trace on the position degrees of freedom, and using the normalization of

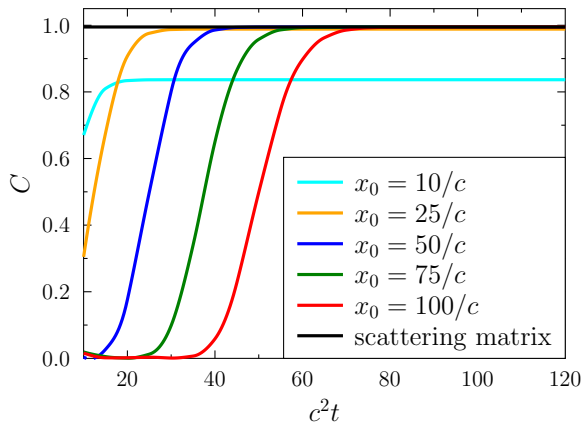


Figure 3: Concurrence as a function of time for different values of the initial position, and as predicted from the scattering matrix formalism ($C \approx 0.995$). We used $\sigma_x = 10/c$ and $p_{AB} = c$.

the wave-function in both symmetric and anti-symmetric subspaces we find that the concurrence is $C = |\Im[\int dy \psi_t^-(y)^* \psi_t(y)]|$.

We consider now two distant Gaussian wavepackets, centered around positions $x_1 = -x_0/2$ and $x_2 = x_0/2$, with width $\sigma_x/\sqrt{2}$, and propagating with speed $v > 0$ and $-v$ respectively, so that the relative momentum is $p_{AB} = -2v$. If $x_0 \gg \sigma_x$, and $vt - x_0 \gg \sigma_x$, then we can assume that the particles are non interacting, both initially and at time t . With this assumption we can perform the integral in Eq. (7) analytically by substituting $|x| \approx x$ and $|y| \approx -y$. Then, the concurrence can be calculated exactly. From the solution, we find that the explicit dependence on x_0 and t disappear, without further approximations, and we get the same expression for C as obtained from the scattering matrix formalism. Therefore, the predictions of the scattering matrix formalism, discussed in the previous section, are accurate enough irrespective of c , provided that the initial and final wave-packets are non-overlapping. This is shown explicitly in Fig. 3 where the concurrence is evaluated numerically without approximations. Note that since $\sigma_p \propto (\sigma_x)^{-1}$ the optimal conditions are $x_0 \gg \sigma_x \gg c^{-1}$ and $p_{AB} = c$.

2.3 Implementation via flying qubits

One of the most promising implementation of our gates is with neutral bosonic/fermionic atoms. The delta function interaction we use is, in fact, very realistic and realizable for neutral

atoms under strong 1D confinement [60]. ^{87}Rb atoms have already been strongly confined to 1D atomic waveguides leading to delta interactions [38]. For ^{87}Rb , with a 3D scattering length $a \simeq 50 \text{ \AA}$ an axial (for 1D) confinement of $\omega_\perp \simeq 100 \text{ kHz}$ gives (using e.g. Refs.[60, 61]) $c \simeq 10^6 \text{ m}^{-1}$. Velocities of atoms in 1D waveguides (*c.f.* atom lasers [44]) can be mm s^{-1} , which translates to $p_{AB} \simeq 10^6 \text{ m}^{-1}$ (in units of wavenumbers). Thereby, $p_{AB} \approx c$ for *optimal gates* is achievable in current technology [62]. Deviation from the 1D effective δ -potential are expected when the condition $p_{AB} \ll \sqrt{\hbar\mu\omega_\perp}$ is not satisfied (where μ is the atomic mass). In that case the scattering matrix has still the form Eq.(5) where c shows a (weak) dependence on p_{AB} [60]. The optimal gate is then found by solving $p_{AB} = c(p_{AB}) \simeq c - \zeta_{3/2}(\mu\omega_\perp/\hbar)^{-3/2} (cp_{AB}/4)^2$, where ζ is the Riemann zeta function. State independent waveguides for two spin states have been met [45] in magnetic waveguides (trivially possible in optical waveguides/hollow fibers). Our gate will be an extension of collision experiments between different spin species [63] with pairs of atoms at a time. Launching exactly two atoms towards each other in 1D should be feasible with microtrap arrays [1, 2, 64] or in atom chips [39, 40] and is also a key assumption in many works [11, 41, 42, 43]. For example, our gates can be made with the technique of Ref.[41] whereby atoms are trapped initially in potential dips inside a larger well and let to roll towards each other in a harmonic potential to acquire their momenta (note that our gate scheme is completely different from Ref.[41], where the atomic motion is guided by internal states). The initial position of the particles $x_B = -x_A = x_0$ can be tailored so that their relative momentum has minimum variance Δp_{AB} when the particles reach the collision point ($x=0$). As $\omega_z \ll \omega_\perp$ (where ω_z is the frequency of the longitudinal harmonic confinement) the collision does not feel the longitudinal potential, so it is approximated by Eq.(5). As shown previously, the generated entanglement is very high ($C \simeq 1$) provided that $\eta \sim \Delta p_{AB}/p_{AB} \sim \Delta x_0/x_0 \ll 1$. A different approach (depicted in Fig. 1b) consists in suddenly moving the local trapping potentials so that the particles in A and B move towards their new potential minima. As in the previous case, wavepackets with well-defined and tunable momenta

are created by switching off the potential when they reach the minima where their momentum uncertainties are minimal.

3 Quantum gates between distant stationary qubits

A discrete variant of the system with a δ -interaction is the Hubbard Hamiltonian [65, 37]:

$$H = \sum_{j,\alpha} \frac{J_j}{2} [a_{j,\alpha}^\dagger a_{j+1,\alpha} + \text{h.c.}] + \sum_{j,\alpha,\beta} \frac{U_j^{\alpha\beta}}{2} n_{j,\alpha} n_{j,\beta}, \quad (9)$$

where $\alpha = \{\uparrow, \downarrow\}$ labels two internal degrees of freedom of the particles. We call N the length of the chain. In a lattice setup, free-space evolution is replaced with particle hopping. Particle collisions lead to a scattering matrix which, for uniform couplings $J_j = J$, $U_j^{\alpha\beta} = U^{\alpha\beta}$, is given by Eq.(3) with the substitutions [65, 66]

$$p_j \rightarrow \sin p_j, \quad c \rightarrow U^{\alpha\beta}/J. \quad (10)$$

A maximally entangling gate is therefore realized when $\sin p_1 - \sin p_2 \approx 2U$, with $U = U^{\uparrow\downarrow}/(2J)$. In particular, $p_1 = \sin^{-1} U$ when $p_2 = -p_1$.

The Hubbard Hamiltonian (9) naturally models cold bosonic/fermionic atoms in optical lattice [67]. Owing to single atom addressing techniques [68] ^{87}Rb atoms in different lattice sites can be initialized in either two distinguishable hyperfine internal states $|\downarrow\rangle \equiv |F=1, m_F=-1\rangle$ and $|\uparrow\rangle \equiv |F=2, m_F=-2\rangle$. The coupling constants $U_j^{\alpha\beta}$ depend on the strength $g_{\alpha\beta}$ of the effective interaction between cold atoms [69]. These parameters are usually experimentally measured [71, 70] and can be tuned by Feshbach resonances [72]. Spin-exchange collisions are highly suppressed due to the little difference (less than 5%) between singlet and triplet scattering length of ^{87}Rb [67]. The one-dimensional regime is obtained by increasing the harmonic lattice transverse confinement ($\omega_\perp/2\pi \approx 18$ kHz see [47, 73] for typical values). We obtain the 1D pseudo-potential coupling constants $g_{\alpha\beta}$ from the 3D measured values [71] following [60], respectively $g_{\uparrow\uparrow} = 1.14 \times 10^{-37}$ J m, $g_{\uparrow\downarrow} = 1.12 \times 10^{-37}$ J m, $g_{\downarrow\downarrow} = 1.09 \times 10^{-37}$ J m. The internal spin state and the position of particles are detected by fluorescence microscopy techniques [68, 74]. The

parameters $U_j^{\alpha\beta}$ and J_j can be physically controlled in optical lattice systems locally varying the depth of the optical potential [75]. Arbitrary optical potential landscapes are generated directly projecting a light pattern by using holographic masks or micromirror device [6, 74]. In particular, $U^{\alpha\beta} \simeq \sqrt{2\pi} (g_{\alpha\beta}/\lambda) (V_0/E_R)^{1/4}$ and $J_j \simeq (4/\sqrt{\pi}) E_R (V/E_R)^{3/4} \exp[-2(V/E_R)^{1/2}]$ where λ is the laser wavelength, V_0 is the lattice depth and E_R is the recoil energy [69].

For flying qubits, in Sec. 2 we considered a fixed c and we tuned p_j to obtain the desired gate. In a lattice, on the other hand, $U_{\alpha\beta}$ can be controlled precisely, while the creation of a wave-packet requires the control and initialization of many-sites. This kind of control can be avoided by initially placing two particles at the two distant boundaries of the lattice (particle A on the left and particle B on the right) and locally tuning the coupling J_0 between the boundaries and the rest of the chain [76] (all the other couplings are uniform $J_j = J$). An optimal choice of J_0/J has a twofold effect [76]: firstly it generates two wave-packets whose momentum distribution is Lorentzian, narrow around $p_A = -p_B \simeq \pm\pi/2$, respectively, and with a width dependent on J_0 ; secondly it generates a quasi-dispersionless evolution, allowing an almost perfect reconstruction of the wave-packets after the transmission (occurring in a time $\approx N/J$) to the opposite end. In this scheme (shown in Fig. 1c), the particles start from opposite locations, interact close to the center of the chain and then reach the opposite end where the wave-function is again almost completely localized, allowing a proper particle addressing. Since $p_{A/B}$ is fixed, a high amount of entanglement is generated when $U = |\sin p_{A/B}| = 1$. For ^{87}Rb we found that the latter condition is satisfied, *e.g.*, when $V_0/E_R \simeq 2.2$, giving also $J/h \simeq 240$ Hz.

In this scheme there are two error sources. The first is due to the transmission quality, though it is above 85% even for long chains [76]. The second one is due to the finite width of the Lorentzian momentum profile around $|p| = \pi/2$ which, in turn, yields slightly different gates for different momentum components. To quantify the amount of these errors we evaluate numerically the joint probability amplitude $A_{ij}^{\alpha\beta}(\tilde{t})$ to have respectively particle A in sites i and particle B in j as function of the inter-particle inter-

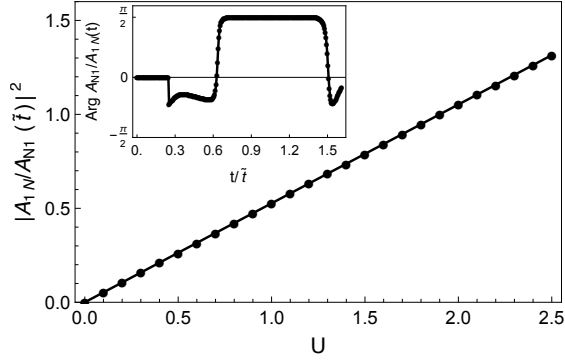


Figure 4: Ratio between the probabilities $|A_{1N}^{\uparrow\downarrow}(t)|^2$ and $|A_{N1}^{\uparrow\downarrow}(t)|^2$ as a function of the interaction parameter $U \equiv U^{\uparrow\downarrow}$ (in units of J), evaluated at the gate time $\tilde{t} \simeq 26.08/J$. The chain length is $N = 21$ and U is set to the optimal value $U = 2U^{\text{opt}} = 2 \times 0.95$. (inset) Phase difference between the amplitude probability $A_{1N}^{\uparrow\downarrow}(t)$ and $A_{N1}^{\uparrow\downarrow}(t)$ as a function of the time t/\tilde{t} .

actions U . The indices α, β refer to the initial internal state of particles A and B , \tilde{t} is the transfer time, and the initial condition is $A_{1N}^{\alpha\beta}(0)=1$. As shown in Fig. 4, we find $A_{1N}^{\uparrow\downarrow}/A_{N1}^{\uparrow\downarrow}(\tilde{t}) = -iU/U_{\text{opt}}$ for distinguishable particles, where U_{opt} is the value of $U^{\uparrow\downarrow}$ that optimises the transformation (5) at time \tilde{t} . This optimal value is found numerically via a linear fit over the data, and it slightly differs from the analytic prediction $U_{\text{opt}}=1$ because of finite size effects. More precisely, in the inset of Fig. 5 we show that U_{opt} scales with the length of the chain N , towards the value $U_{\text{opt}} \rightarrow 1$, in agreement with the analytical prediction. For indistinguishable particles we obtain that $A_{11}^{\alpha\alpha}/A_{1N}^{\alpha\alpha}(\tilde{t})$ is zero for $\alpha=\uparrow, \downarrow$ and for any value of $U^{\uparrow\downarrow}/J$. Therefore, apart from a global damping factor due to the non-perfect wave-packet reconstruction, the resulting transformation is in agreement with the gate (5), with the substitution (10) and $p_1 \simeq \pi/2$.

The entanglement generation between the boundaries is evaluated via the concurrence [56] $C_{1N}(\tilde{t}) = 2|A_{1N}^{\uparrow\downarrow}(\tilde{t})A_{N1}^{\uparrow\downarrow*}(\tilde{t})|$. From the asymptotic analysis [76], since the wavepackets are peaked around $p_j \simeq \pm\pi/2$, we find that

$$C_{1N} = f_{1N}^4 \frac{2U/U_{\text{opt}}}{(U/U_{\text{opt}})^2 + 1}, \quad (11)$$

where f_{1N} is the transmission probability from site 1 to site N at the transmission time and $1 - U_{\text{opt}} \propto \Delta^2$, where Δ is the width of the wave-packet. For optimal values [76] of

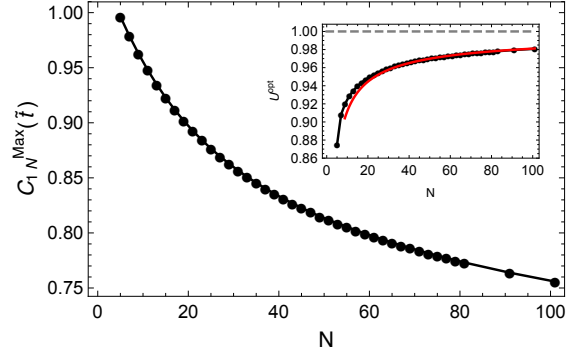


Figure 5: Scaling of the maximum of concurrence as a function of the chain length L . (inset) Optimal inter-particle interaction strength U^{opt} as a function of the chain length N . The numerical value is found via a linear fit over the data of ratio $|A_{1N}^{\uparrow\downarrow}/A_{N1}^{\uparrow\downarrow}|(\tilde{t})$ as a function of the inter-particle interaction, $U \equiv U^{\uparrow\downarrow}/J$. The red line is the fit function $1 - 0.41N^{-2/3}$ over the data.

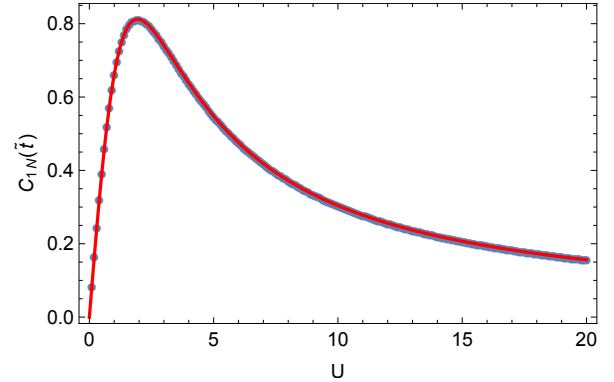


Figure 6: Concurrence as a function of $U=U^{\uparrow\downarrow}/J$ and the prediction (11), for a chain of length $N=51$. The maximal concurrence $f_{1N}^4=0.81$ appears for when $U=U_{\text{opt}}=0.97$.

$J_0 \approx 1.03N^{-1/6}$ one finds $\Delta \simeq 0.53N^{-1/3}$ and accordingly $U_{\text{opt}} \approx 1 - 0.41N^{-2/3}$, as shown in the inset of Fig. 5. On the other hand, the maximum value of the concurrence, shown in Fig. 5, depends only on the transfer quality f_{1N} , which is different from zero even in the thermodynamic limit [76] $f_{1N} \gtrsim 0.847$ for any N . Therefore, in the thermodynamic limit the maximal concurrence is $C = f_{1\infty}^4 \approx 0.5144$. Explicit results for the dependence of the concurrence upon the interaction $U \equiv U^{\uparrow\downarrow}/J$ of a finite chain are shown in Fig. 6.

Finally, in Fig. 7 we consider the effect of noise, in the form of static random local energy shifts in different sites added to the Hamiltonian (9),

$$H_{\text{noise}} = \sum_{j,\alpha} \mu_j n_{j,\alpha}, \quad (12)$$

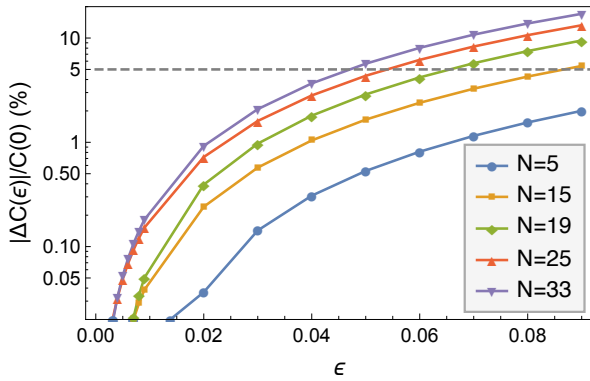


Figure 7: Relative variation $|\Delta C(\epsilon)|/C(0)$ of the concurrence between sites $(1,N)$ at transfer time, under random diagonal noise with strength ϵ . Several chain lengths N are considered. The gray dashed line represents a threshold of the 5%.

where $\mu_j = Jx_j$, with $x_j \in [-\epsilon, \epsilon]$ is a uniform random distribution and ϵ is the perturbation strength. We compute the relative variation of the concurrence with respect to the zero noise case, namely $|\Delta C(\epsilon)|/C(0)$, where $\Delta C(\epsilon) \equiv C_{1N}^{\max}(\tilde{t}, \epsilon) - C_{1N}^{\max}(\tilde{t}, 0)$. As it is clear from the figure, our mechanism is robust against imperfections of $\epsilon \lesssim 0.05$ for a $L = 33$ chain.

4 Concluding remarks

We have proposed a low control method to generate quantum gates from collision, which are necessary building blocks for neutral atom based quantum computation. In view of the recent unprecedented capabilities of observing atomic quantum walks in lattice experiments [6, 5], we show how to use the *natural* interaction between atoms for quantum logic. Our scheme is stable against imperfections and enables the realization of quantum gates by minimizing the need of external control sources. In optical lattice scenarios, our scheme is compelling for applications, as the lattice depth control makes possible to interchange static to flying qubits, avoiding the necessity to seek some mechanism to couple static to mobile particles. At the root of our proposal there is the exploitation of Bethe-Ansatz techniques and quantum indistinguishability. Compared to other recent proposals for quantum logic in 1D [77, 78, 79], our method is more scalable, as it can use the machinery of integrable models, such as the Yang-Baxter relation, to realize composite operations between multiple par-

ticles (see also [80, 81]). Indeed, since in integrable models all complex n -body scattering effects can be factorized into two-body S matrices, one can straightforwardly apply our findings also in multi-particle scenarios.

Acknowledgements:– VK acknowledges financial support by NSF Grant No. DMS-1205422. SB, LB and EC acknowledge financial support from the European Research Council under the European Union’s Seventh Framework Programme (FP/2007-2013) / ERC Grant Agreement No. 308253.

References

- [1] C. Muldoon, L. Brandt, J. Dong, D. Stuart, E. Brainis, M. Himsforth, A. Kuhn, *New J. Phys* **14**, 073051 (2012).
- [2] M. Schlosser, J. Kruse, C. Gierl, S. Teichmann, S. Tichelmann, G. Birkl, *New J. Phys.* **14**, 123034 (2012).
- [3] D. Barredo *et al.*, *Phys. Rev. Lett.* **114**, 113002 (2015).
- [4] M. Saffman, *J. Phys. B: At. Mol. Opt. Phys.* **49** 202001 (2016).
- [5] T. Fukuhara *et al.*, *Nature* **502**, 7679 (2013).
- [6] P.M. Preiss, R. Ma, M.E. Tai, A. Lukin, M. Rispoli, P. Zupancic, Y. Lahini, R. Islam, M. Greiner, *Science* **347**, 1229 (2015).
- [7] D. Greif *et al.*, *Science* **351**, 953 (2016).
- [8] R. Bücker, J. Grond, S. Manz, T. Berrada, T. Betz, C. Koller, U. Hohenester, T. Schumm, A. Perrin, J. Schmiedmayer, *Nature Physics* **7**, 608611 (2011).
- [9] E. Knill, R. Laflamme and G. Milburn, *Nature* **409**, 46 (2001).
- [10] C. W. J. Beenakker, D. P. DiVincenzo, C. Emary, and M. Kindermann, *Phys. Rev. Lett.* **93**, 020501 (2004).
- [11] S. Popescu, *Phys. Rev. Lett.* **99**, 250501 (2007).
- [12] L. -M. Duan and H. J. Kimble, *Phys. Rev. Lett.* **92**, 127902 (2004).
- [13] D. G. Angelakis, M. F. Santos, V. Yannopoulos and A. Ekert, *Phys. Lett. A.* **362**, 377 (2007).

- [14] K. Nemoto and W. J. Munro, Phys. Rev. Lett **93**, 250502 (2004).
- [15] A. Reiserer, N. Kalb, G. Rempe, S. Ritter, Nature **508**, 237240 (2014).
- [16] A. V. Gorshkov *et al.*, Phys. Rev. Lett. **105**, 060502 (2010).
- [17] S. Bose and D. Home, Phys. Rev. Lett. **88**, 050401 (2002).
- [18] F. Ciccarello *et al.*, New J. of Phys. **8**, 214 (2006); F. Ciccarello *et al.*, Phys. Rev. Lett. **100**, 150501 (2008).
- [19] L. Lamata and J. Leon, Phys. Rev. A **73**, 052322 (2006).
- [20] D. S. Saraga, B. L. Altshuler, D. Loss, and R. M. Westervelt, Phys. Rev. B **71**, 045338 (2005).
- [21] P. Samuelsson, E. V. Sukhorukov, and M. Bttiker, Phys. Rev. B **70**, 115330 (2004).
- [22] G. Burkard, D. Loss, E. V. Sukhorukov, Phys. Rev. B **61**, R16303(R) (2000).
- [23] G. Coudourier-Maruri *et al.*, Phys. Rev. A **82**, 052313 (2010).
- [24] M. Lewenstein, B. A. Malomed, New J. Phys. **11**, 113014 (2009).
- [25] D. Loss and D. P. DiVincenzo, Phys. Rev. A **57**, 120 (1998).
- [26] D. Jaksch *et al.*, Phys. Rev. Lett. **85**, 2208 (2000).
- [27] O. Mandel *et al.*, Nature **425**, 937 (2003).
- [28] R. Stock, I. H. Deutsch and E. L. Bolda, Phys. Rev. Lett. **91**, 183201 (2003).
- [29] D. Hayes, P. S. Julienne and I. H. Deutsch, Phys. Rev. Lett. **98**, 070501 (2007).
- [30] M. Anderlini *et al.* Nature **448**, 452 (2007).
- [31] L. Isenhower *et al.*, Phys. Rev. Lett. **104**, 010503 (2010); T. Wilk *et al.*, Phys. Rev. Lett. **104**, 010502 (2010).
- [32] J. Hofmann *et al.*, Science **337**, 72 (2012).
- [33] J.I. Cirac and P. Zoller, Phys. Rev. Lett. **74**, 4091 (1995).
- [34] T. P. Spiller *et al.*, New J. Phys. **8**, 30 (2006).
- [35] L. Banchi, A. Bayat, P. Verrucchi, and S. Bose, Phys. Rev. Lett. **106**, 140501 (2011).
- [36] X. Z. Zhang, Z. Song, Sci. Rep. **6**, 18323 (2016).
- [37] V.E. Korepin, N.M. Bogoliubov and A.G. Izergin, Quantum Inverse Scattering Method and Correlation Functions, Cambridge University Press, 1993; Eq.1.11, pg 5.
- [38] T. Kinoshita *et al.*, Science **305**, 1125 (2004); B. Paredes *et al.*, Nature **429**, 277 (2004); S. Hofferberth *et al.*, Nature Phys. **4**, 489 (2008).
- [39] A. H. van Amerongen *et al.*, Phys. Rev. Lett. **100**, 090402 (2008).
- [40] T. Betz *et al.*, Phys. Rev. Lett. **106**, 020407 (2011); R. Bucker *et al.*, Nature Physics **7**, 608 (2011).
- [41] T. Calarco *et al.*, Phys. Rev. A **61**, 022304 (2000).
- [42] D. Jaksch, H.-J. Briegel, J. I. Cirac, C. W Gardiner, P. Zoller, Phys. Rev. Lett. **82**, 1975 (1999).
- [43] E. T. Owen, M. C. Dean, and C. H. W. Barnes, Phys. Rev. A **85**, 022319, (2012).
- [44] W. Guerin *et al.*, Phys. Rev. Lett. **97**, 200402 (2006).
- [45] P. Wicke, S. Whitlock, and N. J. van Druten, arXiv:1010.4545v1 (2010).
- [46] M. J. Davis, P. B. Blakie, A. H. van Amerongen, N. J. van Druten, and K. V. Kheruntsyan, Phys. Rev. A **85**, 031604(R) (2012).
- [47] J. Catani *et al.*, Phys. Rev. A **85**, 023623 (2012).
- [48] G. Pagano, M. Mancini, G. Cappellini, P. Lombardi, F. Schfer, H. Hu, X.-J. Liu, J. Catani, C. Sias, M. Inguscio, L. Fallani, Nature Physics **10**, 198201 (2014).
- [49] M. Boll, T. A. Hilker, G. Salomon, A. Omran, J. Nespolo, L. Pollet, I. Bloch and C. Gross, Science **353**, 1257 (2016).
- [50] P. Zupancic, P. M. Preiss, R. Ma, A. Lukin, M. Eric Tai, M. Rispoli, R. Islam, and M. Greiner, Opt. Expr. **24**, 13881 (2016).
- [51] C. Weitenberg: Fluorescence Imaging of Quantum Gases. In Quantum Gas Experiments, vol. Volume 3 of Cold Atoms, pp. 121-143 (Imperial College Press) (2014).

- [52] M. J. Bremner *et al.* Phys. Rev. Lett. **89**, 247902 (2002).
- [53] Here energy $E = p_1^2 + p_2^2$.
- [54] C. N. Yang, Phys. Rev. Lett. **19**, 1312 (1967).
- [55] $|\uparrow\rangle_A|\downarrow\rangle_B \equiv a_{p_A,\uparrow}^\dagger a_{-p_B,\downarrow}^\dagger|0\rangle$ ($|0\rangle$ is vacuum) are *rewritten* second quantized notations used commonly for identical flying qubits (*c.f.* [17]).
- [56] W. K. Wootters, Phys. Rev. Lett. **80**, 2245 (1998).
- [57] L. Amico, A., Osterloh, F., Plastina, R., Fazio, G. M Palma, Physical Review A, **69**(2), 022304, (2004).
- [58] M. Abramowitz and I.A. Stegun, *Handbook of Mathematical Functions*, (Dover, New York, 1972), page 298.
- [59] B. Gaveau, L. S. Schulman, Journal of Physics A: Mathematical and General, **19**(10), 1833, (1986).
- [60] M. Olshanii, Phys. Rev. Lett. **81**, 938 (1998).
- [61] L. Rutherford, J. Goold, Th. Busch and J. F. McCann, Phys. Rev. A **83**, 055601 (2011).
- [62] Even outside this regime, the gates are still entangling and thereby useful unless we are at the free ($p_A + p_B \gg c$) or impenetrable ($p_A + p_B \ll c$) limits.
- [63] A. Sommer, M. Ku, G. Roati and M. W. Zwierlein, Nature **472**, 201 (2011).
- [64] F. Nogrette, H. Labuhn, S. Ravets, D. Barredo, L. Béguin, A. Vernier, T. Lahaye, and A. Browaeys, Phys. Rev. X **4**, 021034 (2014).
- [65] M. Gaudin, *The Bethe Wavefunction*, Cambridge University Press (2014)
- [66] W. Krauth, Phys. Rev. B **44**, 9772(R) (1991).
- [67] M. Lewenstein, A. Sanpera, V. Ahufinger, *Ultracold Atoms in Optical Lattices*, Oxford University Press (2012)
- [68] C. Weitenberg *et al.*, Nature **471**, 319 (2011).
- [69] D. Jaksch, C. Bruder, J. I. Cirac, C. W. Gardiner, and P. Zoller, Phys. Rev. Lett. **81**, 3108 (1998).
- [70] J. Weiner *et al.*, Rev. Mod. Phys. **71**,1 (1999).
- [71] M. Egorov *et al.*, Phys. Rev. A **87**, 053614 (2013).
- [72] A. Marte *et al.*, Phys. Rev. Lett. **89**, 283202 (2002) .
- [73] I. Bloch, Nature **1**, 23 (2005).
- [74] W. S. Bakr, J. I. Gillen, A. Peng, S. Fölling, M. Greiner, Nature **462**, 74 (2009).
- [75] D. Jaksch, P. Zoller, Ann. Phys. **315**, 52 (2005)
- [76] L. Banci, T. J. G. Apollaro, A. Cuccoli, R. Vaia, P. Verrucchi, New. J. Phys **13**, 123006 (2011).
- [77] Yoav Lahini, Gregory R. Steinbrecher, Adam D. Bookatz, Dirk Englund, arXiv:1501.04349 .
- [78] E. Compagno, L. Banci, and S. Bose, Phys. Rev. A **92**, 022701 (2015).
- [79] E. Compagno, L. Banci, C. Gross, S. Bose, Phys. Rev. A **95**, 012307 (2017).
- [80] Y. Zhang, Quantum Inf Process, **12**:631 (2013).
- [81] Y. Zhang, Quantum Inf Process, **11**:585 (2012).